X-ray determination of the 1×3 reconstruction of Pt(110)

I. K. Robinson and P. J. Eng
Department of Physics, University of Illinois, Urbana, Illinois 61801

C. Romainczyk* and K. Kern
Ecole Polytechnique Fédérale, CH-1015 Ecublens, Switzerland
(Received 25 November 1992)

We have carried out a detailed structure determination of the 1×3 reconstructed Pt(110) surface, using three-dimensional x-ray-diffraction data. Since the ground state of Pt(110) is a 1×2 structure, a small amount of chemical contamination is required to produce the 1×3 state. It is, however, reproducible both in our experiment and in other laboratories. The structure contains a double missing row that exposes the fourth layer. Relaxations are substantial with the largest displacements in the fourth and fifth layers. The results are compared with theoretical predictions of surface contraction due to cohesion.

INTRODUCTION

The missing-row 1×2 reconstructions of Au(110) and Pt(110) are among the most accurately determined of all surface structures. Recent independent studies by low-energy electron diffraction (LEED) (Ref. 1) and x-ray diffraction[2] now agree with each other within their experimental error bars. The LEED study[1] has a higher stated precision than the x-ray study[2] on the vertical coordinates (of 0.02 versus 0.1 Å) but is less accurate horizontally (0.04 versus 0.01 Å); the contrast between these relative sensitivities comes from the volumes of reciprocal space sampled, respectively, by the two techniques.[3] Because this missing-row structure is believed to be very reliable, it has become a benchmark for the detailed testing of theories of the general principles governing surface structure, and there has been much progress along these lines.[4]

It was realized from the earliest investigations with LEED, however, that higher-order structures also exist for both Au(110) and Pt(110): Moritz and Wolf noted a 1×3 structure in their original study of Au(110),[5] although they could not clearly establish the conditions of its formation and state: "it seems to be dependent on the special ion-bombardment conditions and probably on the cooling rate after tempering." On Pt(110), the 1×3 state was first reported by Mundschau and Vanselow,[6] then by Fery, Moritz, and Wolf,[1] Stock et al.[7] and Masson and Rabalais.[8] Three of these studies agreed that the structure was stabilized by a small amount of impurity. The ion-recoil spectroscopy experiment indeed identified Ca and K as impurities.[8] The fourth study by Fery, Moritz, and Wolf[1] found that the 1×3 structure could be obtained by simply heating in oxygen to 1200 K, since subsequent Auger electron spectroscopy (AES) showed the 1×3 sample to be free from contamination. The authors argued further that a low level of impurities, below the detection limit of AES, inevitably must be the origin of the 1×3 structure. Their sample, once in the 1×3 state, always gave 1×3 after further cycles of sputtering and annealing. In fact, it required many cycles of heating to 1800 K to return to the 1×2 state. In other work, heating in oxygen was found to restore the 1×2 structure.[8]

Impurities appear to be involved in the origin of the Au(110) 1×3 structure, as well. Häberle, Fenter, and Gustafsson[5] found that dosing with Cs led to the 1×3 state reproducibly at a coverage Θ of about 5% of a monolayer. They were able to measure the structure with medium-energy ion scattering (MEIS).[9] Held et al.[10] found that a similar crystal of Au(110) produced the 1×3 structure all the time, and they were even able to study its phase transitions. Flynn-Sanders et al.[11] examined K/Au(110) and placed the 1×3 state in the Θ-T phase diagram at about Θ=0.05–0.1. Recently Ocko et al.[12] found that the 1×3 structure was the preferred state of the Au(110)/water interface, at least at certain electrochemical potentials.

Theoretical studies[13,14] have found that for Au(110) and Pt(110), the 1×3 and 1×2 structures indeed have very similar energies, as have other analogous 1×n structures.[14] It is therefore easy to understand why both the 1×3 and 1×2 states are found experimentally, with perhaps a slight chemical (impurity) force driving the balance between them. Here[13,14] it was assumed that the 1×3 structure consisted of a double missing-row arrangement, shown in Fig. 1, with two out of three rows missing in the top layer and one out of three in the second, as was later confirmed by experiments.[1,9] In Au(110) and Pt(110), "double" steps, containing atoms from three atomic layers, can be built from the structure that appears in one half of the 1×3 unit cell (see Fig. 1). The total energy of this configuration was also found to be indistinguishable from those of the 1×3 and 1×2 structures,[15] and indeed these were found to be the elementary excitations of the 1×2 to "1×1" phase transition of Pt(110).[16,17]

In this work, we report the detailed atomic structure of the Pt(110) 1×3 surface obtained by x-ray-diffraction analysis. The results show once again that very high accuracy can be obtained for a large number of unknown
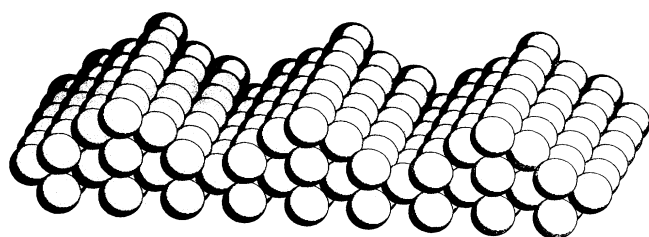
Pt(110) 1×3 Missing Row Structure

FIG. 1. A pictorial view of the 1×3 reconstructed Pt(110) surface.

parameters (atomic positions of eight independent atoms), and that significant conclusions can be drawn regarding the compression of interatomic spacings at the surfaces of noble metals. This is generally in agreement with recent findings for Au(100),[18] Pt(100),[19] Au(111),[20] and Pt(111).[21]

EXPERIMENTAL METHOD

Our sample preparation was a little unusual because the 1×3 structure is not the usual reconstructed state of Pt(110). We attempted first to follow the published recipe of Fery, Moritz, and Wolf[1] to obtain this state without success; it led instead to irreversible faceting of that crystal. Instead we were successful with the recipe published by Masson and Rabalais,[8] which worked reproducibly for our sample: we started with another freshly polished crystal in ultrahigh vacuum (UHV) and subjected it to very light Ar^+ ion sputtering and extensive (several hours) heating at 600 °C, both with and without an oxygen pressure of 10^{-8} Torr. We found that heating in oxygen resulted in a 1×2 structure as determined by LEED and surface x-ray diffraction. Heating in UHV, however, resulted in a well-ordered 1×3 state after some hours, as reported in Ref. 8. The process was found to be reversible, as oxygen treatment restored the 1×2 state, again as reported previously.[8] Small traces (a few percent) of carbon were detectable in the 1×3 surface by AES, while the 1×2 surface was found to be clean. We could not detect any additional contamination, but cannot rule out the possibility of segregation of other species at the present level. Notable possibilities are K and Ca, known bulk impurities in Pt, whose AES lines coincide with minor liners of the Pt itself, but had been previously detected in the Pt(110) 1×3 structure.[8] Fery, Moritz, and Wolf[1] had likewise concluded in their paper that the 1×3 surface must be an impurity-stabilized state of Pt(110), although they could not identify the agent.

The transition from 1×2 to 1×3 was observed *in situ* while the segregation was taking place. We interpreted this in terms of a two-dimensional phase diagram for Pt(110) that will be discussed in a separate publication.[22] The 1×3 state survived cooling down to room temperature, remaining well ordered. The sharp, low background LEED pattern and C-contaminated AES spectrum were unchanged 24 hours later, during which period we were

able to complete the crystallographic measurements necessary to determine the structure of the 1×3 state.

X-ray-diffraction measurements were made at the National Synchrontron Light Source (NSLS), using the X16A beamline which is operated by AT&T Bell Laboratories. Bending magnet radiation was focused by a cylindrical mirror onto a 1.0×1.5-mm spot at the sample 25 m away. In front of the sample, a double Si(111) monochromator selected an x-ray energy of 7.5 keV with a bandpass of about 5×10^{-4}. The Pt sample was mounted on an UHV-compatible five-circle diffractometer described previously.[23] The crystal was aligned by locating two bulk Bragg peaks. A tetragonal indexing convention, hkl_{tet}, was used to allow the 110_{cubic} surface normal to be 001_{tet}, thus spanned by a single Miller index L. 100_{tet} is along the 001_{cubic} direction, while 010_{tet} lies along the in-plane $1\bar{1}0_{cubic}$. This is the same convention used in LEED for fcc(110) surfaces. The direction of the optical surface was determined with a laser beam, and this was used together with the crystallographic alignment to control the angles of x-ray incidence onto and from the surface, and to keep the surface normal in the horizontal plane for good resolution matching.[24] In this way, the crystal miscut was determined to be 0.075° along an azimuth 30° away from the 100_{tet} direction.

Our instrumental resolution was defined by 2-mm slits positioned 600 mm from the sample, just in front of the detector. This gave a resolution width of $w=0.006$ Å^{-1} half width at half maximum (HWHM) in radial scans. The diffraction peaks at $\frac{1}{3}$-order positions were found to be resolution limited, but had more tails than the resolution function. We concluded from the tails that the intrinsic width was probably not much narrower than 0.006-Å^{-1} HWHM, so that the (exponential) coherence length $\xi=1/w$ was not much longer than 180 Å.

CRYSTALLOGRAPHIC MEASUREMENTS

Data were collected at $\frac{1}{3}$-order and integer-order positions by means of rocking scans of the diffractometer ω axis with a wide detector slit.[25] In this way, the integrated intensities of the peaks could be obtained after background subtraction. The intensities were corrected for the Lorentz factor, the active sample area defined by the entrance and exit slits, and the small polarization effect associated with the α axis.[26] All available symmetry equivalents of the reflections shown in Fig. 2 were measured and averaged together. The variation among strong reflections was 9%, which was used as our error of observation. A total of 313 data gave 95 inequivalent structure factor values, covering 27 in-plane positions and the L dependence sampled along 14 rods. The radii of the left semicircles in Fig. 2 are the observed values obtained. Out-of-plane data at $L=0.8$ are shown along the dotted axes below the $L=0.05$ values.

Dramatic variations of intensity are evident along the rods: most reflections have structure factors ranging from close to zero to some quite large value between $L=0$ and 0.8, i.e., 100% modulation along the rod. Some examples of the full profile are shown in Fig. 3. The maximum range available is an instrumental limitation linked to the
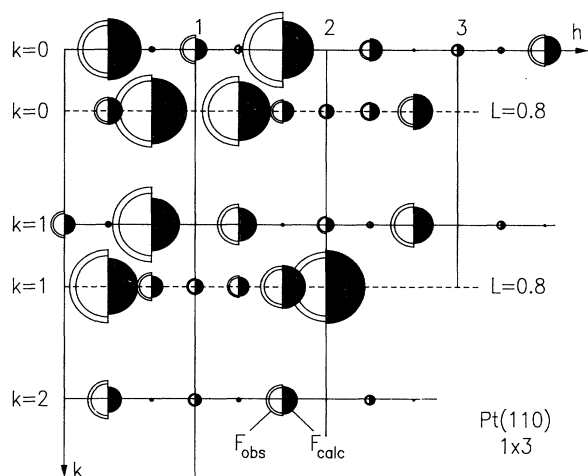
FIG. 2. Observed and calculated intensities for the 1×3 structure of Pt(110) for in-plane ($L=0.05$, solid grid) and out-of-plane ($L=0.8$, dashed grid) slices of reciprocal space. Error bars ($\pm\sigma$) are indicated for the observed values. The calculation is for the best fit described in the text.

size of the Be window,[23] which allows incident angles only up to 45°. The modulation means the structure is very clearly *not* two-dimensional, and must have substantial structure in at least two atomic layers, such as featured in the double missing row in Fig. 1. This is the most dramatic example of "three-dimensional" behavior seen to date with the surface x-ray technique: up to 50% modulation of rod structure factors has been observed previously in Au(110) 1×2 (Ref. 2) and W(001) $\sqrt{2}\times\sqrt{2}$ structures,[27] which both have substantial second-layer displacements.
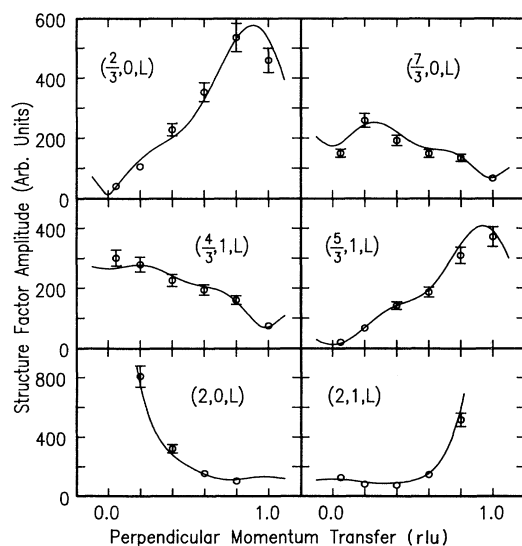

FIG. 3. A selection of rod profiles with best-fitting calculated curves for the measurements of the Pt(110) 1×3 structure.

CRYSTALLOGRAPHIC ANALYSIS

The ultimate aim of the data analysis is to obtain a satisfactory least-squares agreement factor χ^2. The utility of quoting χ^2 values is that they measure the disagreement in units of the experimental error of the data, which is known;[25] when χ^2 drops to unity, no further information can be extracted. However, it should be noted that χ^2 is not a good index for comparing one structure determination with another that is based on different data. We started our data analysis by testing the double missing-row model. Allowing no displacements of the individual atoms, we fitted a scale factor and overall Debye-Waller (DW) factor and obtained a least-squares residual χ^2 of 16.6. This already shows considerable agreement, in that the general sense of the rod modulations was reproduced, so it was concluded that the double missing-row structure was an appropriate guess for a starting model. The model suggested by Masson and Rabalais,[8] with two missing rows in the top layer and none in the second, gave bad agreement with $\chi^2=49$.

Next, we introduced the displacements in the double missing-row structure determined by Fery, Moritz, and Wolf,[1] listed in Table I, and obtained $\chi^2=9.4$. The displacements in the 1×3 structure of Cs/Au(110) measured by MEIS,[9] also listed in Table I, gave $\chi^2=11.4$ when the DW factor was allowed to vary, and much worse when this was fixed at the experimental value of 1.4 Å^2. Thus either of these models was an improvement on the double

TABLE I. Atomic displacements in Å for the best-fit model of the Pt(110) 1×3 structure. The labels refer to Fig. 4, with the thermal B parameters (defined as $B=8\pi^2\langle u^2\rangle$) numbered according to the atom number. The final χ^2 for this model was 2.63. MEIS data refer to a medium-energy ion-scattering study of Cs/Au(110) that also has the same 1×3 reconstruction (Ref. 9). Values corresponding to blank entries were not determined.

	X ray (this work)	LEED (Ref. 1)	MEIS (Ref. 9)
x_2	0.014(5)	0.04	$-0.04(4)$
x_3	0.019(4)	0.01	
x_6	0.029(5)		
x_7	0.045(4)		
z_1	$-0.08(3)$	-0.18	$-0.34(6)$
z_2	$-0.05(3)$	0.11	$-0.16(4)$
z_3	0.10(3)	0.18	0.03(4)
z_4	0.26(2)	0.04	
z_5	$-0.02(3)$	0.00	$-0.11(4)$
z_6	$-0.05(2)$	-0.01	
B_1	4.1(4) Å^2		
B_2	3.4(3) Å^2		
B_3	2.7(3) Å^2		
B_4	2.4(3) Å^2		1.4(4) Å^2
B_5	3.0(3) Å^2		
B_6	2.6(3) Å^2		
β	0.07(2)		
f	0.89(1)		

missing row without relaxation. On the other hand, when the displacements and DW factors were all allowed to vary under least-squares refinement, we obtained a substantial improvement and a final χ^2 of 2.6. The parameters obtained are listed in Table I under the "x-ray" column.

The calculated structure factors are shown alongside the observations in Fig. 2 for comparison. Examples of calculated rod profiles are shown in Fig. 3, passing through the data as well. Clearly the strong intensity modulation is reproduced. Included in the data set are several "integer-order" reflections which contain bulk contributions in the form of crystal truncation rods (CTR's),[28] arising from the termination of the bulk lattice. The characteristic divergence of the intensity is seen along these rods approaching the bulk Bragg peaks at $L = 1$ or 0, depending on the parity. As these data were included in the analysis, it was necessary to include a "surface fraction" parameter f in the fitting.[29] f represents the fraction of the surface that appears to be reconstructed; the remainder is assumed to contribute to the CTR's but not the fractional-order data. The final value $f = 89\%$ is not much less than unity, suggesting a well-prepared surface. An additional refinement parameter associated with fitting CTR's is the roughness β, representing the fraction of the surface area (within one coherence area) where the lattice starts at a different height.[28] $\beta = 7\%$ corresponds to an root-mean-square roughness of only 0.39 Å.

DESCRIPTION OF MODEL

The displacement parameters x_i and z_i and DW parameters B_i listed in Table I belong the ith atom denoted in Fig. 4. The mirror planes marked in the figure, as well
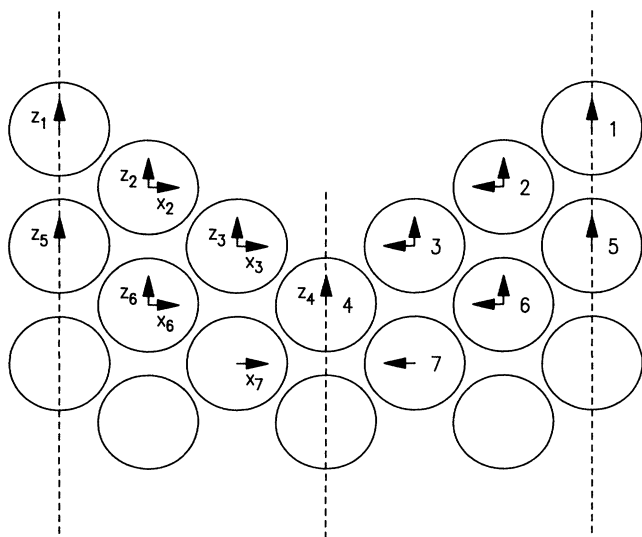

FIG. 4. The final model of the Pt(110) 1×3 structure. The dashed lines represent assumed mirror symmetries of the unit cell. Atom numbers are defined for reference, as are the symmetry-allowed displacement parameters used in fitting. The arrows indicate the positive displacement directions, not the displacements themselves.

as mirrors at $y = 0$ and $\frac{1}{2}$, are the assumed symmetries of the structure. All $p2mm$ symmetry-allowed displacements have been included in the top four layers, along with the x_7 parameter in the fifth layer.

There is a clear trend of an increasing DW parameter with height in the structure; the outermost layer has 4.1 Å^2, the next 3.4 Å^2, the third layer an average of 2.9 Å^2, and the fourth 2.5 Å^2. All of these values are rather large compared with other structures; the corresponding values for the Pt(110) 1×2 structure (measured in the same way) were, for example, 1.5 Å^2 for the outermost layer and 1.4 Å^2 for the second layer.[2] To understand the significance of this, it is important to note that the classical DW model cannot distinguish between thermal vibration and static disorder. We do expect *local* disorder to be present because of the impurities, and a root-mean-square (rms) displacement of 0.23 Å does not seem impossibly large for a 5% impurity coverage. The trend of the DW factor with height is expected regardless of whether its origin is thermal vibration or static disorder. The values we observe are substantially larger than the MEIS value[9] of 1.4 Å^2; this is not suprising, because that technique really measures *relative* positions of one layer with respect to the one below, and so does not see the effects of correlations due either to vibration or static disorder. The ramping of vibration amplitude with height was also seen in a study of Au(100),[18] and this became a large effect at high temperatures.

The vertical displacement parameters z_i also show a clear trend. The outer two layers are relaxed inwards, while the third and fourth layers are buckled: atoms 3 and 4 move out but 5 and 6 move inwards. Atom 4 has the largest displacement in the whole structure, even though it is in the fourth layer. The most dramatic effect of this is to compact the 111_{cubic} facet made up of atoms 1–4. The interatomic spacings are all compressed, 1 and 2 by 0.2%, 2 and 3 by 2.7%, and 3 and 4 by 3.1%; the effective atomic densities are compressed by the same amounts. The horizontal displacements x_i have a related trend, *increasing* from the top to the bottom of the structure; they are all directed toward the missing row, just as they are in the Pt(110) 1×2 structure.[2] The largest displacement, of atom 7, partially fills the gap left by the outward motion of atom 4, but still leaves a 4–7 interatomic distance 3.9% longer than the bulk. The x_i magnitudes are generally a little smaller than the 0.05 and 0.04 Å for the second and fourth layers in the Pt(110) 1×2 structure.

SURFACE COMPRESSION

Our results agree with LEED (Ref. 1) in the sense that they identify the same double missing-row model. At the more detailed level, there is not such good agreement in the structural parameters themselves, unlike the case of the Pt(110) 1×2 surface with its simpler structure. Because of the inclusion of integer-order data, our derived vertical coordinates are referenced to deep inside the bulk crystal; the LEED coordinates are referenced (arbitrarily) to the surface because of the limited penetration of electrons. Much, but not all, of the apparent discrepancy in z_i is due to this choice of origin. This is less serious in

the comparison of interlayer spacings. The same is true to a lesser extent of the comparison with MEIS. A unique aspect of the x-ray method is this bulk point of reference. The result that the fourth layer moves so far outwards is therefore a result that is new to this study.

The interatomic spacings around the atoms of the top two layers are under compression; this is the expected behavior of metal atoms with low-coordination sites: atoms 1 and 2 have coordinations of 7 and 9, respectively. Deeper down, the atoms have almost full coordination shells (of 12 neighbors), and we find a mixture of expansions and compressions, with the largest bondlength expansion being 9% beneath atom 4 (though this is somewhat less reliable since the fifth-layer heights were not refined) and the largest compression being 3.1%. The *average* compression of the seven neighbors of atom 1 is 0.6%, and that of the nine neighbors of atom 2 is 0.7%; the corresponding values in the LEED study[1] were 3.1% and 0.1%.

ORIGINS OF COMPRESSION

To understand the significance of these changes, it is useful to consider a theoretical model of metallic bonding which includes the effects of electronic cohesion and its relation to coordination. The basic origin of surface compression was proposed by Finnis and Heine[30] as being due to the core's electrostatic response to the "smoothing" of electron density at the surface. A specific model was developed for Au by Ercolessi, Tosatti, and Parrinello,[31] and we will assume that its qualitative aspects will also apply to Pt, which has analogous surface behavior. Pt has a higher Debye temperature, and so has 33% smaller bulk vibration amplitudes and 38% smaller thermal expansion, but this is explained quite well by the same potential functions. The model is related to "effective-medium" descriptions that have been successful elsewhere for Cu and Al.[32] The form of the potential energy is given by[31]

$$V = \frac{1}{2} \sum_{j \neq i} \phi(|r_i - r_j|) + \sum_i U(n_i) , \qquad (1)$$

where the first term is a conventional two-body potential and the second term depends on the total effective number of neighbors n_j surrounding each atom. n_j is given by

$$n_j = \sum_{j \neq i} \rho(|r_j - r_i|) ,$$

where $\rho(r_j - r_i)$ is a softened weighting function that has value unity for a normal (bulk) neighbor distance and value zero beyond the first coordination shell. The functions ϕ, U, and ρ were obtained for bulk gold using various known bulk physical properties, and are graphed in Ref. 31.

According to these potential functions, there would be an cohesive energy cost of 1.5 eV per atom from the U term (in the absence of relaxation) for an atom with a coordination of 7, and a cost of 0.65 eV for an atom with a coordination of 9. This is the driving force for compression. We illustrate this point by calculating the

dependence of the energy, V, on the average bond length for different values of the coordination in Fig. 5. From this, we can estimate the ideal relaxation expected around surface atoms with lower coordination. Specifically, we find that atom 1 would have a minimum in energy if there were an average compression of 7.8% of its seven neighbor distances, and that atom 2 (nine neighbors) would be at a minimum with 4.5% average compression.

Our experimental values for the compression are an order of magnitude smaller than this theory would suggest. Furthermore, the same statement is true of the compressions seen in this structure with LEED.[1] Part of the reason for the disagreement is the effect of temperature: Table I shows relatively large values for the temperature factors, B_i, corresponding to root-mean-square (rms) vibration amplitudes of 0.23 and 0.21 Å, respectively, for atoms 1 and 2. From Fig. 5, we can estimate the effects of anharmonicity in the vibrations using the same effective-medium potentials.[31] We find a contribution to the surface thermal expansions of 0.047 (1.6%) and 0.043 Å (1.5%), respectively. These values represent a thermal expansion coefficient of 5.5×10^{-5} K^{-1}, or six times the bulk value. Such a proposal is not out of the question, since similar surface enhancements of thermal expansion have been reported by others.[33] A related argument could be constructed to explain how static disorder due to impurities could cause local expansions that would partially cancel the compression. Therefore, we propose that the effects of cohesive compression would be counteracted by anomalous thermal expansion of the surface.

Other related surface structures can be used to compare compression trends. Au(110) and Pt(110) 1×2 structures have been widely studied, and have average compressions of the seven-coordinated top layer (exactly analogous to atom 1 in Fig. 4) ranging from 2.6% to
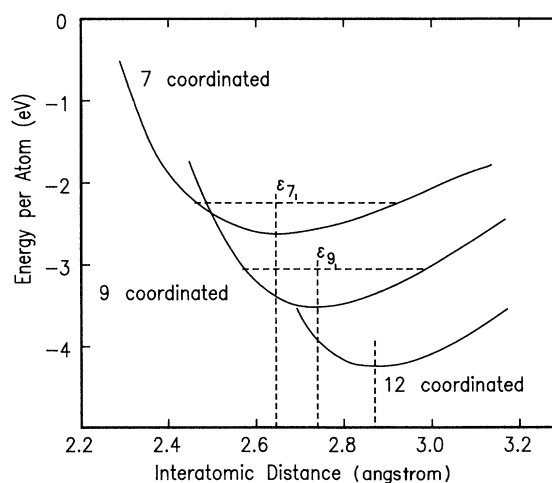

FIG. 5. Theoretical effective interatomic potentials calculated from the semiempirical "glue" model of Ercolessi, Tosatti, and Parrinello (Ref. 31) for different numbers of equidistant Au-Au neighbors, using Eq. (1). The compression of the shell and enhanced anharmonicity are clearly seen for the lower coordinations.

3.8%;[1−3,5] a first-principles total-energy theory gave 2.7% for the Au(110) 1×2 structure.[4] In these experiments, anharmonicity effects are insignificant, so the contractions would be expected to be around 7.8%. Similarly, the average compressions observed[34] in Au(100) (1.3%) and Au(111) (0.3%) are also smaller than the 4.5% value expected for their effective coordination numbers of 9. In Au(100), a 1.4% anharmonicity contribution would be expected because the rms vibration amplitude is 0.19 Å.[34]

Second, the contractions seen in this structure are smaller than expected even in comparison with the other structures mentioned. Third, the refined values of Debye-Waller factors are larger than expected and show a clear trend, decreasing with depth. Both these last points may be reconciled with the known presence of impurities in the surface: the large B_i parameters would include some (static) disorder rather than just thermal effects, and this disorder would give rise to local perturbations in the structure that reduce the average compression.

CONCLUSIONS

We can make several general conclusions in addition to confirming the double missing-row structure of the Pt(110) 1×3 surface. First, the semiempirical potentials given by Ercolessi, Tosatti, and Parrinello[31] overemphasize the compression that arises from cohesive forces, since the large weight of experimental (and first-principles theory) favors values one third as large.

ACKNOWLEDGMENTS

*Also at IGV-KFA Jülich, Germany.

[1]P. Fery, W. Moritz, and D. Wolf, Phys. Rev. B **38**, 7275 (1988).

[2]E. Vlieg, I. K. Robinson, and K. Kern, Surf. Sci. **233**, 248 (1990).

[3]I. K. Robinson, E. Vlieg, and K. Kern, Faraday Discuss. R. Soc. Chem. **89**, 159 (1990).

[4]K. M. Ho and K. P. Bohnen, Europhys. Lett. **4**, 345 (1987); K. M. Ho and K. P. Bohnen, Phys. Rev. Lett. **59**, 1833 (1987).

[5]W. Moritz and D. Wolf, Surf. Sci. **88**, L29 (1979).

[6]M. Mundschau and R. Vanselow, Phys. Rev. Lett. **53**, 1084 (1984).

[7]M. Stock, J. Risse, U. Korte, and G. Meyer-Emsen, Surf. Sci. **233**, L243 (1990).

[8]F. Masson and J. W. Rabalais, Surf. Sci. **253**, 258 (1991).

[9]P. Häberle, P. Fenter, and T. Gustafsson, Phys. Rev. B **39**, 5810 (1989).

[10]G. A. Held, J. L. Jordan-Sweet, P. M. Horn, A. Mak, and R. J. Birgeneau, Solid State Commun. **72**, 37 (1989).

[11]D. K. Flynn-Sanders, K. D. Jamison, J. V. Barth, J. Winterlin, P. A. Thiel, G. Ertl, and R. J. Behm, Surf. Sci. **253**, 270 (1991).

[12]B. M. Ocko, G. Hegelsen, B. Schardt, J. Wang, and A. Hamelin, Phys. Rev. Lett. **69**, 3350 (1992).

[13]S. M. Foiles, Surf. Sci. **191**, L779 (1987).

[14]F. Ercolessi, A. Bartolini, M. Garofalo, and E. Tosatti, Surf. Sci. **189/190**, 636 (1987).

[15]L. D. Roelofs, S. M. Foiles, M. S. Daw, and M. I. Baskes, Surf. Sci. **234**, 63 (1990).

[16]I. K. Robinson, E. Vlieg, and K. Kern, Phys. Rev. Lett. **63**, 2578 (1989).

[17]J. Villian and I. Vilfan, Surf. Sci. **199**, 165 (1988).

[18]D. Gibbs, B. M. Ocko, D. M. Zehner, and S. G. J. Mochrie, Phys. Rev. B **42**, 7330 (1990).

[19]D. Gibbs, G. Grübel, D. M. Zehner, D. L. Abernathy, and S.

G. J. Mochrie, Phys. Rev. Lett. **67**, 3117 (1991).

[20]K. G. Huang, D. Gibbs, D. M. Zehner, A. R. Sandy, and S. G. J. Mochrie, Phys. Rev. Lett. **65**, 3313 (1990).

[21]A. R. Sandy, S. G. J. Mochrie, D. M. Zehner, G. Grübel, K. G. Huang, and D. Gibbs, Phys. Rev. Lett. **68**, 2192 (1992).

[22]I. K. Robinson, P. J. Eng. C. Romainczyk, and K. Kern (unpublished).

[23]P. H. Fuoss and I. K. Robinson, Nucl. Instrum. Methods **222**, 171 (1984).

[24]E. Vlieg, J. F. van der Veen, J. E. Macdonald, and M. Miller, J. Appl. Cryst. **20**, 330 (1987).

[25]I. K. Robinson in *Handbook on Synchrotron Radiation,* edited by D. E. Moncton and G. S. Brown (North-Holland, Amsterdam, 1991), Vol. III, Ch. 7, pp. 221–266.

[26]I. K. Robinson, D. M. Smilgies, and P. J. Eng, J. Phys. Condens. Matter **4**, 5845 (1992).

[27]M. S. Altman, P. J. Estrup, and I. K. Robinson, Phys. Rev. B **38**, 5211 (1988).

[28]I. K. Robinson, Phys. Rev. B **33**, 3830 (1986).

[29]E. Vlieg, Ph.D. dissertation, FOM Institute, Amsterdam, 1987.

[30]M. W. Finnis and V. Heine, J. Phys. F **4**, L37 (1974).

[31]F. Ercolessi, E. Tosatti, and M. Parrinello, Phys. Rev. Lett. **57**, 719 (1986).

[32]K. W. Jacobsen, J. K. Nørskov, and M. J. Puska, Phys. Rev. B **35**, 7423 (1987).

[33]Y. Cao and E. H. Conrad, Phys. Rev. Lett. **65**, 2808 (1990); J. W. M. Frenken and J. F. van der Veen, *ibid.* **54**, 134 (1985).

[34]D. L. Abernathy, D. Gibbs, G. Grübel, K. G. Huang, S. G. J. Mochrie, B. M. Ocko, A. R. Sandy, and D. M. Zehner, in *Surface X-Ray and Neutron Scattering,* edited by H. Zabel and I. K. Robinson (Springer-Verlag, Heidelberg, 1992), p. 37.